Inhibition of Stat3 by a Small Molecule Inhibitor Slows Vision Loss in a Rat Model of Diabetic Retinopathy

Phillip A. Vanlandingham,[1] Didier J. Nuno,[1] Alexander B. Quiambao,[1] Eric Phelps,[1] Ronald A. Wassel,[1,2] Jian-Xing Ma,[3] Krysten M. Farjo,[3] and Rafal A. Farjo[1,2]

[1]Charlesson LLC, Oklahoma City, Oklahoma, United States
[2]EyeCRO, LLC, Oklahoma City, Oklahoma, United States
[3]Department of Physiology, University of Oklahoma Health Sciences Center, Oklahoma City, Oklahoma, United States

Correspondence: Rafal A. Farjo, EyeCRO, LLC, 800 Research Parkway, Suite 360, Oklahoma City, OK 73104, USA;
rfarjo@eyecro.com.

Submitted: August 29, 2016
Accepted: February 19, 2017

Citation: Vanlandingham PA, Nuno DJ, Quiambao AB, et al. Inhibition of Stat3 by a small molecule inhibitor slows vision loss in a rat model of diabetic retinopathy. *Invest Ophthalmol Vis Sci*. 2017;58:2095–2105. DOI: 10.1167/iovs.16-20641

Purpose. Diabetic retinopathy is a leading cause of vision loss. Previous studies have shown signaling pathways mediated by Stat3 (signal transducer and activator of transcription 3) play a primary role in diabetic retinopathy progression. This study tested CLT-005, a small molecule inhibitor of Stat3, for its dose-dependent therapeutic effects on vision loss in a rat model of diabetic retinopathy.

Methods. Brown Norway rats were administered streptozotocin (STZ) to induce diabetes. CLT-005 was administered daily by oral gavage for 16 weeks at concentrations of 125, 250, or 500 mg/kg, respectively, beginning 4 days post streptozotocin administration. Systemic and ocular drug concentration was quantified with mass spectrometry. Visual function was monitored at 2-week intervals from 6 to 16 weeks using optokinetic tracking to measure visual acuity and contrast sensitivity. The presence and severity of cataracts was visually monitored and correlated to visual acuity. The transcription and translation of multiple angiogenic factors and inflammatory cytokines were measured by real-time polymerase chain reaction and Multiplex immunoassay.

Results. Streptozotocin-diabetic rats sustain progressive vision loss over 16 weeks, and this loss in visual function is rescued in a dose-dependent manner by CLT-005. This positive therapeutic effect correlates to the positive effects of CLT-005 on vascular leakage and the presence of inflammatory cytokines in the retina.

Conclusions. The present study indicates that Stat3 inhibition has strong therapeutic potential for the treatment of vision loss in diabetic retinopathy.

Keywords: diabetic retinopathy, signal transducer and activator of transcription 3, inflammation, optokinetic tracking

Diabetes mellitus (DM) affects more than 300 million people worldwide, with that number expected to almost double during the next 20 years.[1] The majority of individuals with DM will develop DR leading to severe vision loss; therefore DR is now a major health concern.[2,3] Despite established strategies to slow disease progression, none are shown to be effective in preventing long-term vision loss.[4,5]

Preclinical indications of DR primarily consist of the onset of visual deficits, including a progressive inability to distinguish contrast in the visual field.[6,7] Clinical signs of DR include abnormal blood vessel growth, blood vessel leakage, and retinal cell death.[8–12] Major risk factors include diabetes-related hyperglycemia, hypertension, dyslipidemia, oxidative stress, and inflammation.[11,13–20]

The traditional standard of care for DR is laser photocoagulation, but newer therapeutics that include corticosteroids and anti-VEGF antibodies have resulted in improved patient outcomes.[21–23] The most effective of these is the use of anti-VEGF antibodies, and there are several new VEGF inhibitors currently in clinical trials.[24] However, many patients do not respond to the anti-VEGF agents, and there remains a need for new drugs that can serve as a second-line therapy.[25]

Stat3 is a critical mediator of signaling pathways that regulate both physiology and pathology of the retina, and therefore provide a primary target for therapeutic intervention. Stat3 is present as an inactive monomer in the cytosol of most cell types. Following activation by phosphorylation, the Stat3 monomers dimerize and translocate to the nucleus, where it upregulates transcription of numerous genes in multiple cell signaling pathways.[26–29] Direct and indirect inhibition of Stat3 is protective in multiple inflammation-linked ocular diseases.[30–33] Furthermore, inhibition of VEGF attenuates pathologic retinal angiogenesis in a Stat3-dependent manner.[34] Multiple studies definitely link Stat3 activity with DR disease progression. First, retinal Stat3 mRNA and protein levels are elevated in diabetic rat retinas.[35] Second, inhibition of Stat3 decreases retinal cell death in a rat model of diabetes[36] and decreases retinal inflammation in a mouse model of Type I diabetes.[37] Furthermore, nicotinamide adenine dinucleotide phosphate (NADPH)-oxidase inhibitors and statins protect against oxidative stress related DR pathology through inactivation of Stat3.[38,39]

The administration of STZ causes pancreatic β-cell death, resulting in DM, and is a commonly used method to induce DR in multiple species.[40,41] STZ-induced DR recapitulates many

aspects of the human disease, such as thickening of the capillary basement membrane, dysfunction and apoptosis of retinal cells, increased vascular permeability, and loss of pericytes in retinal capillaries.[42–46] More recent reports have demonstrated DR-associated vision loss in STZ-diabetic rodents using optokinetic tracking (OKT) to measure visual function.[47–50]

To address the involvement of Stat3 in DR, we tested the cell permeable small molecule Stat3 inhibitor, CLT-005. CLT-005 binds with high affinity to the src-homology 2 (SR2) domain of Stat3 and prevents dimerization, nuclear translocation, and DNA binding.[51,52] In this study, we investigated the effect of CLT-005 on diabetes-induced vision loss in STZ-induced diabetic Brown Norway (BN) rats. We found that both visual acuity and contrast sensitivity were improved by CLT-005 administration in a dose-dependent manner. The rescue of vision loss corresponds to a reduction in retinal levels of activated Stat3 and multiple inflammatory cytokines. This ability of CLT-005 to ameliorate vision loss can be separated from a secondary effect on rescuing cataract formation. Therefore, our data suggest that inhibition of Stat3-mediated inflammation in the retina is a promising therapeutic strategy to prevent diabetes-related vision loss.

Materials and Methods

Formulation Preparation and Storage

Drug and vehicle formulations were prepared to ensure that the gavage volume did not exceed 10 ml/kg/animal weekly. CLT-005 was weighed and added to corn oil, and the mixture was then sonicated continuously for 5 minutes at a setting of 40% using a probe sonicator (Vibra Cell Model VCX 750 from Sonics & Materials, Inc., Newtown, CT, USA). To ensure drug stability, all formulations were stored protected from light at room temperature and monitored daily for potential precipitation.

Animal Housing

Age-matched female BN rats (6–8 weeks) weighing between 126 to 137 grams were obtained from Charles River Laboratories, Inc. (Wilmington, MA, USA) and randomly assigned to different treatment groups. For the vascular permeability and RT-PCR data only, four groups of four rats per group were used. For all other data, six groups of six rats per group were used. All animals were housed under standard animal care conditions. The animals were maintained under normal cyclical light conditions consisting of 12 hours of light (<500 lux) followed by 12 hours of darkness. The treatment of animals conformed to the ARVO Statement for the Use of Animals in Ophthalmic and Vision Research and was approved by the University of Oklahoma Health Science Center's Institutional Animal Care and Use Committee.

STZ Injection and Glucose Measurement

The animals were acclimated for 1 week prior to STZ injection. On the day prior to injection, the rats were weighed and baseline blood glucose measurements were taken via tail vein bleed using a OneTouch Glucose Monitoring System (Johnson & Johnson, New Brunswick, NJ, USA). Following an overnight fast, the rats were administered 50 mg/kg of STZ in 10 mM sodium citrate, pH 4.5, intraperitoneally. Nonfasting blood glucose was again measured 3 days post STZ administration to check for hyperglycemia (blood glucose concentration $\geq$ 250 mg/dL). Nonfasting blood glucose levels were monitored weekly for the duration of the study. All blood glucose measurements were individually recorded according to an established animal identification system.

Anesthesia and Euthanasia

An anesthesia cocktail was prepared at a ratio of 1 part Ketamine (100 mg/mL) and 5 parts Xylazine (20 mg/mL) and administered at 1 μL/g of body weight via intraperitoneal injection using a 0.3 cc insulin syringe, 12-mm 30 G needle.

Evans Blue

The vascular permeability assay was performed with Evans blue as tracer following a documented protocol.[53] Anesthetized rats were administered Evans blue dye (30 mg/kg body weight) via injection through the femoral vein under microscopic inspection. After injection, the rats were kept on a warm pad for 2 hours to ensure the complete circulation of Evans blue dye. The chest cavity was then opened, and the rats were perfused via the left ventricle with 1× PBS (pH 7.4), which was prewarmed to 37°C to prevent vasoconstriction. Immediately after perfusion, the eyes were enucleated and the retinas were carefully dissected under an operating microscope. The Evans blue dye was extracted in formamide by sonication and centrifugation. The Evans blue dye was then quantified by absorbance measurement at 420 nm and normalized to the total amount of retinal protein present in the harvested samples.

Quantitative Real-Time PCR

Total RNA was isolated and purified from the posterior segment tissue samples using the TRIzol Plus RNA Purification Kit (Invitrogen, Inc., Carslbad, CA, USA) and was eluted in a total volume of 30 μL. PCR was performed as previously described.[54]

Insulin Implantation

Linplant sustained release insulin implants (Linshin Canada, Inc., Toronto, Ontario, Canada) were used to treat STZ-induced diabetic rats with glucose levels above 250 mg/dL with exogenous insulin. A 16 G disposable hypodermic needle was used to pierce the skin, and the insulin implant was placed subcutaneously on the upper abdomen via a trocar. Glucose was monitored weekly, and if the blood glucose elevated above 250 mg/dL, a second round of surgical insulin implantation was performed.

Oral Gavage

The animals were gavaged once daily beginning at 3 days post STZ injection and continuing for the duration of the study. For each group, the gavage volume was 10 μL/g of body weight. An 18 G 3″ curved feeding needle (Cadence Science, Cranston, RI, USA) attached to a 3-mL Luer lock syringe was placed in the animal's mouth and advanced via the esophagus to the stomach, where the drug was dispensed.

Optokinetic Tracking

Visual function was measured using a virtual OKT system (OptoMotry, Cerebral Mechanics, Inc., Medicine Hat, Alberta, Canada) designed for rapid, quantifiable behavioral measurements of spatial vision in a virtual environment.[55] The animals were placed on a platform surrounded by four computer monitors forming a square inside an enclosed box. The monitors displayed continuous vertical sine wave gratings

Investigative Ophthalmology & Visual Science

rotating across the monitors at 12 deg/s, which appeared to the animal as a virtual three-dimensional rotating cylinder. The animal's ability to visualize the sine wave was monitored via a video camera positioned directly above the animal to display an image perpendicular to the animal's field of vision. The rotation of the virtual cylinder was constantly centered at the animal's viewing position to ensure a consistent viewing distance. Tracking movements were identified as slow, steady head movements in the direction of the rotating grating. All measurements of contrast threshold were performed at a spatial frequency threshold of 0.064 cycle/deg. The contrast sensitivity was calculated as a reciprocal of the Michelson contrast from the screen's luminance (maximum − minimum)/(maximum + minimum) and plotted on a log scale.

Cataract Scoring

Following anesthesia and eye dilation, images of the rat lens were taken using an Amscope 0.3MP Aptima Camera attached to an upright brightfield Amscope microscope (Amscope, Irvine, CA, USA), and Toupview software (Version 3.7, Zhejiang, China). Cataracts were scored on a scale established by Muranov et al.[48,56] as follows: 0 = clear lens, no opacity; 1 = opaque tendril formation apparent at the central nucleus of the lens; 2 = complete opaque coverage of lens nucleus with opaque formation spreading to the lens perimeter; 3 = the majority of the lens has become opaque, but total lens coverage still not achieved; 4 = total opacity of the lens.

Tissue and Plasma Collection

A 1-cc syringe with a 26 G 5/8″ needle was used to make a cardiac puncture on the sedated animals. Whole blood was immediately placed in a BD Microtainer tube (Franklin Lakes, NJ, USA) with K_2EDTA (BD no. 365974) and inverted several times. The samples were allowed to sit at room temperature for 15 minutes and then were centrifuged at 1500*g* for 15 minutes at room temperature. The resultant supernatant (plasma) was transferred to a 1.5-ml screwcap tube and stored at −80°C.

For tissue collection, the eyes were dissected to collect the retina alone or the pigment epithelium, choroid, and sclera (PECS) together. The dissected tissue was placed in a sterile screw cap microfuge tube (VWR International, LLC, Radnor, PA, USA), snap frozen in liquid nitrogen, and stored at −80°C.

Pharmacokinetic Analysis

Tissue was homogenized in PBS at a final concentration of 175 mg tissue homogenate/ml in a Bullet Blender Storm 24 (Next Advance, Averill Park, NY, USA). A small volume of the tissue homogenate was then diluted in acetone and an internal standard (ketoprofen). The mixture was vortexed for 5 minutes at room temperature and centrifuged at 3000*g* for 2 minutes. The supernatant was collected and transferred to an HPLC vial and run on an HPLC Agilent 1100 system (Agilent Technologies, Santa Clara, CA, USA). Separation of CLT-005 and ketoprofen was carried out using an EpicC18MS (ES Industries, West Berlin, NJ, USA) column (4.6 × 50 mm, 5 μm) with a 7-minute isocratic elution consisting of 40% water in 0.1% formic acid and 60% 50:50 acetonitrile:isopropyl alcohol in 0.1% formic acid at a flow rate of 500 μL/min. The injection volume was 10 μL. Positive ion electrospray ionization mass spectrometric analysis was carried out using an Applied Biosystems (Foster City, CA, USA) API 3200 QTrap mass spectrometer at unit resolution with collision-induced dissociation and multiple reaction monitoring. The source temperature was 700°C, the electrospray voltage was 5500 V, and the declustering potential was 70 V. Nitrogen was used as the collision gas at 60 eV, and the dwell time was 150 ms/ion. During multiple reaction monitoring, both CLT-005 and ketoprofen were measured by recording the signal for the transition of the deprotonated molecules of *m/z* 267.1 to the most abundant fragment ion of *m/z* 165.2. The multiple reaction monitoring transition of *m/z* 255.12 to 105.1 was monitored for the ketoprofen internal standard. Data were acquired and analyzed using Analyst software version 1.4 (Applied Biosystems).

Immunoblot

At study termination, retinas were individually isolated and snap frozen in liquid nitrogen. Retinal tissue was homogenized by adding 1 scoop of 0.9 to 2.0 mm diameter beads (no. SSB14B; Next Advance, Inc., Averill Park, NY, USA) and 150 μL of cell lysis buffer (Bio Rad, Hercules, CA, USA) to each retina. The tubes were placed in a Next Advance Bullet Blender Storm 24 and homogenized at a speed setting of 12 for 5 minutes at 4°C. The tubes were then removed and rocked for 15 minutes at 4°C and centrifuged at 13,000*g* for 5 minutes at 4°C. The supernatant was removed to a new tube, and a Bradford assay was conducted to determine protein concentration. Equal concentrations of total protein were separated by SDS-PAGE, transferred to PVDF, and detected using either a rabbit polyclonal antibody against phosphorylated Stat3 (catalog [cat.] no. 9145; Cell Signaling, Danvers, MA, USA) or a mouse monoclonal antibody against β-actin (cat. no. A3854; Sigma-Aldrich Corp., St. Louis, MO, USA).

Multiplex Analysis

Eye tissue was homogenized in Cell Lysis buffer (Bio Rad) using a Bullet Blender Storm 24. Protein concentration was measured using a bicinchoninic acid (BCA) assay (Pierce, Waltham, MA, USA) and reconstituted to 5 mg/ml in cell lysis buffer. Cytokine levels were analyzed using a Bio Rad Bio-plex Pro Rat Cytokine Group I 23-Plex Assay according to protocol (cat. no. L8001V11S5).

Statistical Analysis

Statistical analysis of rtPCR and LC/MS data was performed using a Mann-Whitney nonparametric *t*-test. Statistical analysis of OKT and multiplex data was performed using a 1-way ANOVA with Tukey's posttest. All statistical analysis was performed in GraphPad Prism 5.0 (San Diego, CA, USA).

Results

CLT-005 Reduces Retinal Vascular Permeability and mRNA Expression of Proinflammatory and Proangiogenic Molecules in STZ-Diabetic Rats

We first examined the effect of Stat3 inhibition on retinal vascular leakage in STZ-diabetic rats. At 2 weeks post STZ, blood glucose was measured, and hyperglycemic rats received an intravitreal injection of 1 μg or 5 μg of CLT-005 in one eye and the vehicle (DMSO) alone in the contralateral eye. After 7 days, we quantified retinal vascular permeability by the Evans blue extravasation method.[53] We found a significant decrease in retinal vascular permeability in eyes treated with doses as low as 1 μg of CLT-005 (Fig. 1A).

We also examined the effect of Stat3 inhibition on mRNA expression of several pathogenic molecules in STZ-diabetic rats. At 2 weeks post STZ injection, hyperglycemic rats received intravitreal injections of 50 ng or 5 μg of CLT-005 in one eye and vehicle alone in the contralateral eye. At 24 hours

Investigative Ophthalmology & Visual Science

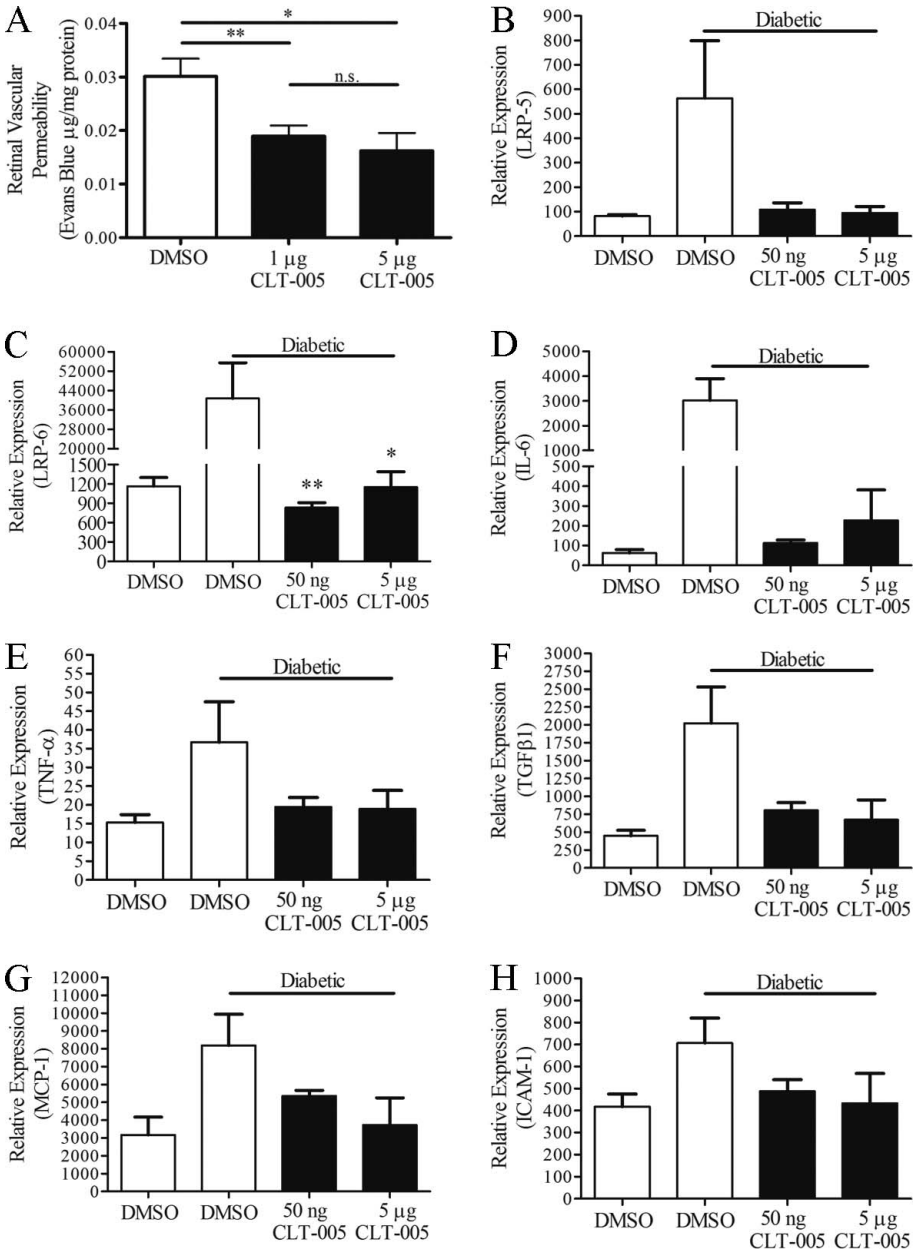

Figure 1. Intravitreal administration of CLT-005 downregulates vascular leakage and angiogenic factor expression in STZ-diabetic rats. (**A–H**) Two weeks following induction of diabetes with STZ, the rats received an intravitreal administration of dimethyl sulfoxide (DMSO) vehicle in one eye, and CLT-005 at the indicated dose in the contralateral eye. (**A**) At 7 days post intravitreal administration, Evans blue-albumin leakage from blood vessels into the retina was quantified as an indication of retinal vascular permeability. Treatment with either 1 µg or 5 µg of CLT-005 significantly decreases retinal vascular leakage relative to vehicle alone. (**B–H**) At 24 hours post intravitreal administration, the retinas were collected and qRT-PCR was used to quantify the mRNA levels of the indicated molecules. Nondiabetic BN rats were also treated with DMSO as an additional control. STZ-diabetic rats show a dramatic increase in gene expression for each of the examined molecules, and treatment with CLT-005 brings transcript levels near nondiabetic levels ($n = 4$; mean ± SEM; $^{*}P < 0.05$; $^{**}P < 0.01$; Mann-Whitney nonparametric *t*-test).

postinjection, the mRNA expression of target molecules was measured by qRT-PCR. Relative to nondiabetic BN rats, the STZ-diabetic rats had an increased expression of the proangiogenic factors LRP-5 and LRP-6, and treatment with CLT-005 dramatically reduced the expression levels in the retina of diabetic rats (Figs. 1B, 1C). Similarly, the proinflammatory molecules IL-6, TNF-α, TGFβ1, monocyte chemotactic protein 1 (MCP-1), and intracellular adhesion molecule 1 (ICAM-1) were upregulated in STZ-diabetic rat retinas, and treatment with either 50 ng or 5 µg of CLT-005 returned the expression of these inflammatory markers to nondiabetic levels (Figs. 1D–H).

Systemic Administration of CLT-005 Is Well Tolerated in STZ-Diabetic Rats

DR is a chronic multifactorial disease, and patients display a gradual decline in visual function following disease onset. To examine the long-term effects of Stat3 inhibition on visual function, BN rats with STZ-induced diabetes were given CLT-005 at 125, 250, or 500 mg/kg/animal or vehicle alone via daily oral gavage for 16 consecutive weeks. Additional controls included a nondiabetic group and STZ-diabetic rats treated with insulin.

Investigative Ophthalmology & Visual Science

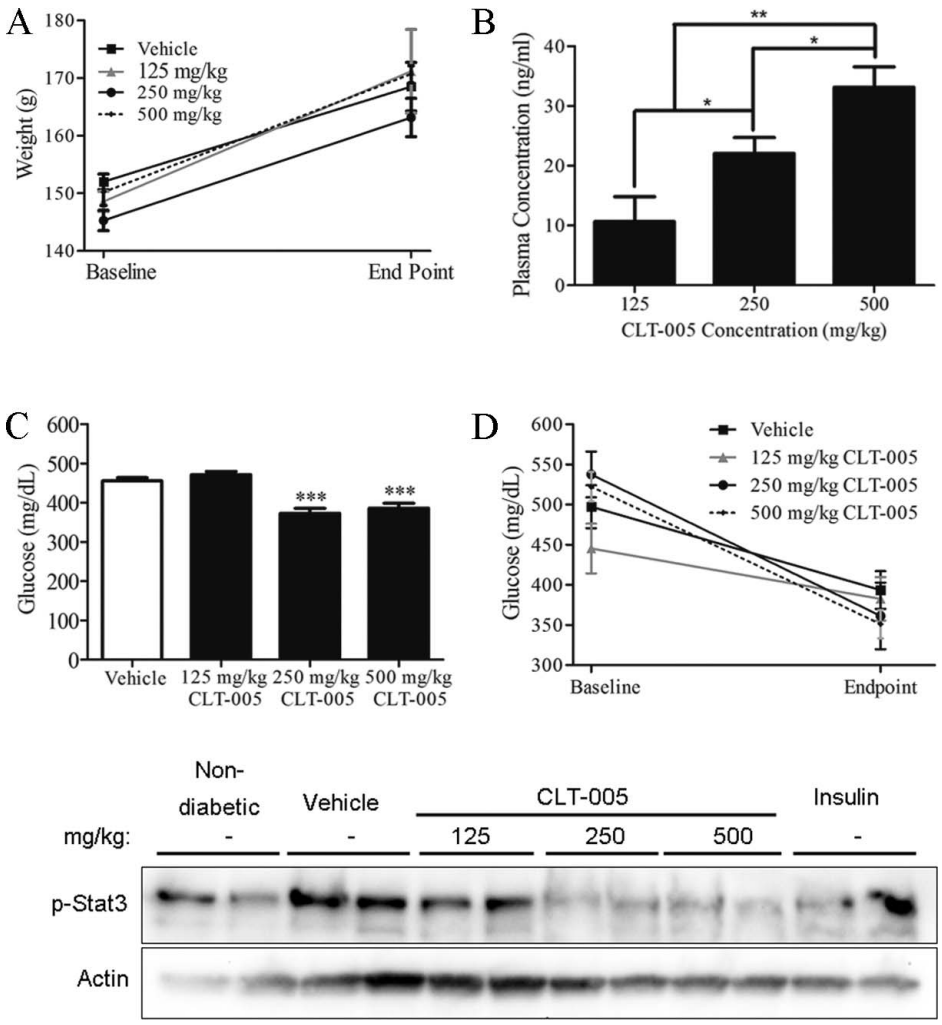

Figure 2. CLT-005 is effectively delivered systemically via oral gavage and is well tolerated by BN rats. (**A**) The baseline (4 days post STZ) and endpoint (16 weeks post STZ) weights were averaged for each group. Daily dosing of CLT-005 did not adversely affect weight gain at week 16 for any of the given doses when compared with the vehicle treatment. (**B**) Following 16 weeks of daily doses, whole blood was collected 3 hours after the terminal dose, and CLT-005 concentration in the plasma was measured by liquid chromatography/mass spectrometry (LC/MS). CLT-005 concentration in the plasma was dose dependent (mean ± SEM; $^{*}P < 0.05$; $^{**}P < 0.01$; Mann-Whitney nonparametric *t*-test). (**C**) Glucose levels were measured once a week for 16 weeks post STZ. All measurements within each group during the duration of the study were averaged and plotted (mean ± SEM). The groups receiving the two highest doses of CLT-005 had significantly lower average blood glucose levels during the course of the study when compared with the animals receiving either vehicle or 125 mg/kg CLT-005 ($^{***}P > 0.001$; Mann-Whitney nonparametric *t*-test). (**D**) The baseline (4 days post STZ) and endpoint (16 weeks post STZ) nonfasting glucose levels were averaged for each group and plotted. The differences between baseline and endpoint glucose levels were greatest for the groups administered the two highest doses of CLT-005. (**E**) Retinas were dissected from animals within the indicated treatment group, and equal concentrations of protein were processed for SDS-PAGE, transferred to polyvinylidene fluoride (PVDF), and immunoblotted with the indicated antibodies. Stat3 activity is higher in the retinas of STZ-diabetic rats treated with vehicle or 125 mg/kg CLT-005 compared to the two highest doses of CLT-005.

During the course of the study, we did not observe abnormal changes in behavior, adverse clinical observations, or mortality (data not shown) related to CLT-005 treatment. Figure 2A shows CLT-005 treatment did not cause body weight loss in STZ-diabetic animals during the course of the study. Pharmacokinetic analysis of whole blood shows CLT-005 is effectively delivered via oral gavage, and systemic drug levels are dose dependent (Fig. 2B). We also measured the nonfasting blood glucose levels in STZ-diabetic animals at weekly intervals. All groups receiving either vehicle or CLT-005 displayed sustained hyperglycemia (blood glucose > 250 mg/dL). However, averaging glucose readings throughout the study within individual groups revealed that animals receiving either 250 or 500 mg/kg CLT-005 had significantly reduced blood glucose levels when compared with the vehicle-treated animals (Fig. 2C). All groups showed an overall downward trend in blood glucose levels during the course of this study, and this downward trend was steepest for animals receiving the two highest doses of CLT-005 (Fig. 2D).

Stat3 activity in the retina was measured at the conclusion of the study. Individual retinas were collected within 3 hours of the final administration of CLT-005 and immediately processed for immunoblot assay. Stat3 activity, as indicated by levels of phosphorylated Stat3, were highest in the vehicle-treated diabetic rats (Fig. 2E). Diabetic rats treated with 250 or 500 mg/kg CLT-005, respectively, had greatly reduced levels of phosphorylated Stat3 when compared with the group treated with 125 mg/kg CLT-005 (Fig. 2E).

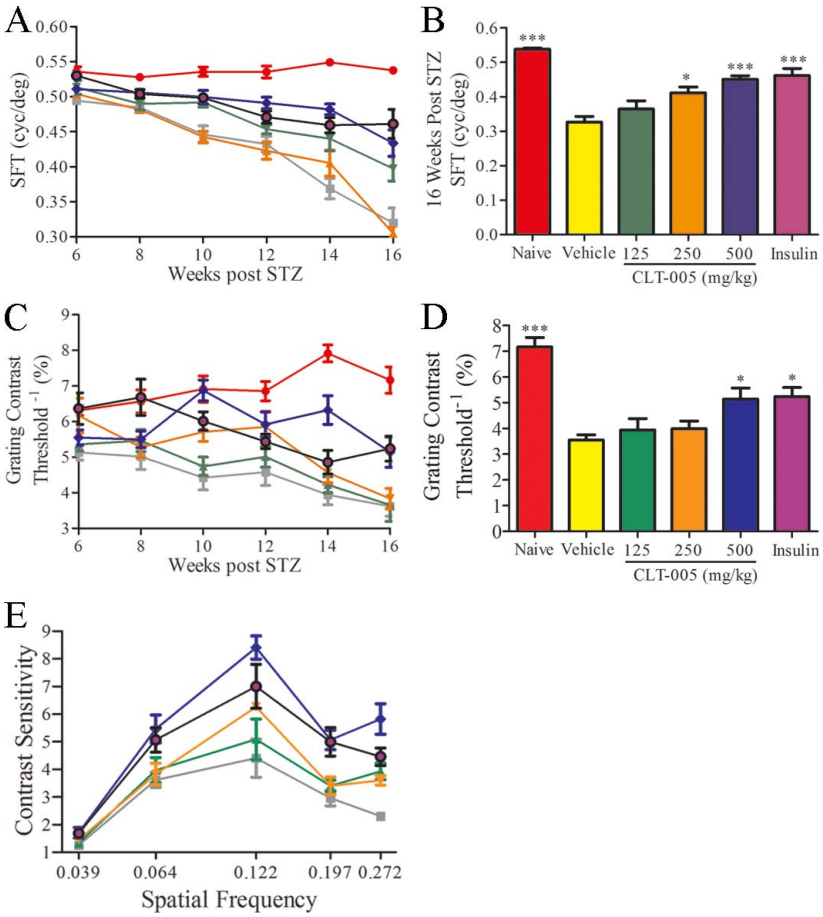

Figure 3. CLT-005 rescues vision loss in STZ-diabetic rats in a dose-dependent manner. (**A**, **B**) OKT was used to measure the SFT values in BN rats at 2-week intervals post STZ. At 6 and 8 weeks post STZ, the SFT values are comparable in all STZ-diabetic groups. However, by week 10, the SFT values significantly diverge between the vehicle and 125 mg/kg CLT-005 groups and the 250 and 500 mg/kg groups. For the 250 mg/kg CLT-005 group, $P < 0.01$ at 10, 14, and 16 weeks when compared with the vehicle group. For the 500 mg/kg CLT-005 group, $P < 0.01$ at 10 weeks, and $P < 0.001$ at 14 and 16 weeks when compared with the vehicle group (1-way ANOVA with Tukey's posttest). (**B**) At 16 weeks post STZ, both the 250 and 500 mg/kg CLT-005 groups have significantly higher SFT values when compared with the vehicle treated group and are not significantly different than the insulin-rescued group (mean ± SEM; $^{*}P < 0.05$; $^{***}P < 0.0001$; 1-way ANOVA with Tukey's posttest). (**C**) OKT was used to measure the contrast thresholds in BN rats at 2-week intervals post STZ. STZ-diabetic animals receiving 500 mg/kg CLT-005 retained their ability to distinguish contrast during the course of 16 weeks at levels comparable to insulin-rescued STZ-diabetic rats. For the 250 mg/kg CLT-005 group, $P < 0.05$ at 10 and 12 weeks when compared with the vehicle group. For the 500 mg/kg CLT-005 group, $P < 0.05$ at 12 weeks, $P < 0.001$ at 10, 14, and 16 weeks when compared with the vehicle group (1-way ANOVA with Tukey's posttest). (**D**) The average contrast threshold values within each group at week 16 were plotted and the values were compared with the vehicle treated group (mean ± SEM; $^{*}P < 0.05$; 1-way ANOVA with Tukey's posttest). The 500 mg/kg CLT-005 group had significantly higher contrast threshold values and is not significantly different than the insulin-rescued group. (**E**) Contrast sensitivity was evaluated as a measure of contrast threshold values at the indicated spatial frequencies at 16 weeks post STZ. STZ-diabetic rats receiving 500 mg/kg CLT-005 have greater contrast sensitivity across spatial frequencies when compared with the other treated STZ-diabetic groups. (**A**, **C**, **E**) *red line*, naive; *gray line*, vehicle; *blue line*, 500 mg/kg CLT-005; *orange line*, 250 mg/kg CLT-005; *green line*, 125 mg/kg CLT-005; *black line*, insulin rescue.

Systemic Delivery of CLT-005 Ameliorates Diabetic Visual Defects in a Dose-Dependent Manner

We used OKT to determine the effect of CLT-005 on vision loss in STZ-diabetic rats. For all groups, visual acuity (spatial frequency threshold [SFT]) and contrast threshold values were determined at 2-week intervals beginning at 4 weeks post STZ and continuing through 16 weeks post STZ. As shown in Figure 3, there was a gradual decline in visual acuity in the vehicle-treated STZ-diabetic rats from week 6 to week 12, and a dramatic loss in visual acuity from week 12 to week 16 post–diabetes onset (Fig. 3A). STZ-diabetic animals that received the lowest dose of CLT-005 (125 mg/kg) showed a declining trend in visual acuity similar to vehicle-treated animals, with no significant difference in SFT values between the two groups. Conversely, STZ-diabetic animals that received the two highest doses of CLT-005 (250 and 500 mg/kg) displayed a delayed decline of visual acuity (Fig. 3A). Furthermore, both high-dose groups had significantly higher SFT values at 16 weeks post STZ relative to vehicle-treated animals ($P < 0.05$ and $P < 0.001$, respectively; Fig. 3B). STZ-diabetic animals that received 500 mg/kg CLT-005 maintained visual acuity levels through 16 weeks post STZ similar to diabetic animals supplemented with insulin (Figs. 3A, 3B).

CLT-005 mediated inhibition of Stat3 also delayed the loss of the STZ-diabetic rat's ability to distinguish contrast in visual stimuli (Fig. 3C). Similar to the time-dependent loss in visual acuity, both vehicle-treated and low-dose CLT-005 treated STZ-diabetic animals showed comparable declines in contrast thresholds. Although the onset of the decline was delayed, STZ-diabetic animals that received 250 mg/kg CLT-005 did not have contrast threshold levels significantly different than the

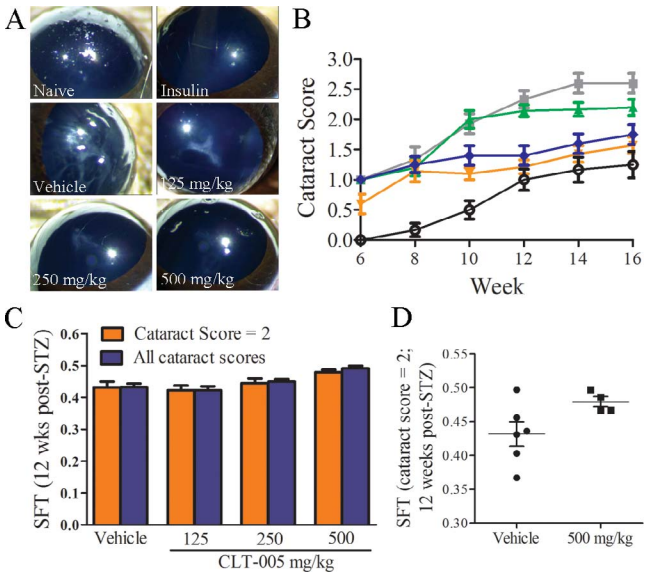

Figure 4. CLT-005 reduces cataract severity and incidence in STZ-diabetic rats. (**A**) Representative images of cataracts from naïve and STZ-diabetic groups. (**B**) Cataracts were scored every 2 weeks beginning at 6 weeks post STZ treatment. The development of severe cataracts (score $>$ 2) was delayed in rats receiving the two highest doses of CLT-005, with the average score remaining lower than the vehicle-treated animals through 16 weeks post STZ. (**C**) The average SFT values from eyes with a cataract score of 2, which represents the upper level of severity at this time point, were separated from the average SFT values of all other eyes within each group and plotted side by side. The data show the SFT values are comparable for different cataract scores within each group. (**D**) Scatterplot representation of each eye with a cataract score of 2 in either the vehicle or 500 mg/kg CLT-005 groups. The data show that even in animals with the same cataract scores across treatment groups, the group receiving 500 mg/kg CLT-005 maintain higher overall SFT values (mean $\pm$ SEM; $^*P < 0.05$; two-tailed paired *t*-test).

vehicle group at 16 weeks post STZ (Figs. 3C, 3D). However, STZ-diabetic animals treated with the highest dose of CLT-005 showed both delayed onset and sustained higher contrast threshold values when compared with all the other diabetic groups (Figs. 3C, 3D). Likewise, the high-dose CLT-005 group had higher contrast threshold values at all observed spatial frequencies (Fig. 3E). Taken together, the acuity and contrast visual threshold data show that CLT-005 ameliorates vision loss in STZ-diabetic rats in a dose-dependent manner.

Correlation Between Cataracts and Visual Deficits in Diabetic BN Rats

Cataract formation correlates to visual deficits in STZ-diabetic Long Evans rats, but are not the sole factor determining vision loss.[48,50] In this study, we imaged and scored cataracts immediately following OKT measurements. Figure 4A shows representative images of cataracts from each group. In both vehicle and CLT-005 treated STZ-diabetic rats, we observed initial cataract formation at 6 weeks post STZ, whereas cataract onset was delayed in insulin-treated rats (Fig. 4B). At 10 weeks post STZ, the relative severity of cataracts between the vehicle and low-dose groups began to diverge from the two high-dose groups, and the cataract scores remained significantly higher on average at all subsequent time points for the vehicle and low-dose groups (Fig. 4B).

We analyzed the relationship between cataract severity and visual function within groups at 12 weeks post STZ. This time point offers the highest degree of variability in cataract scores

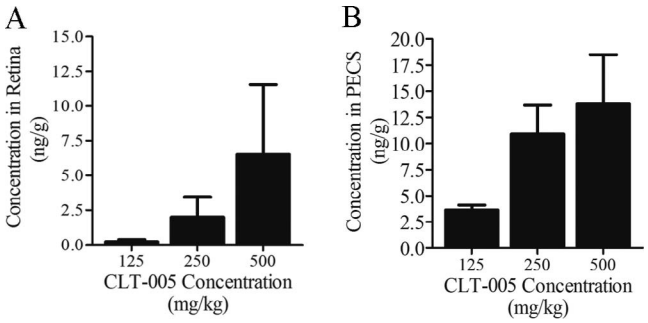

Figure 5. Orally administered CLT-005 is delivered to the eye. LC/MS quantification of CLT-005 in (**A**) retina and (**B**) PECS after daily gavage for 16 weeks at 125, 250, and 500 mg/kg of CLT-005. Eyes were enucleated within 3 hours of final gavage treatment and immediately processed for analysis ($n = 5$, mean $\pm$ SEM).

within the groups, thus allowing us to separate high-grade and low-grade cataracts within each group. The mean SFT is comparable for animals with high-grade cataracts and low-grade cataracts within groups (Fig. 4C). Therefore, although there is a temporal correlation between cataract formation and SFT decline, cataracts are not the sole contributor to the decline. To further confirm this lack of direct causation, we compared animals with a cataract score of 2 across groups at 12 weeks post STZ. The results of this analysis show that the SFT values correlate more strongly with drug dose than with cataract score (Fig. 4D). These data support the conclusion that Stat3 inhibition rescues visual acuity loss at least partly independent of its effect on cataract formation.

CLT-005 Acts Locally to Reduce the Presence of Inflammatory Mediators in the Retina

At the conclusion of the study, retina and PECS tissue were collected separately within 3 hours after the final oral dose and analyzed by mass spectrometry. Pharmacokinetic analysis showed that CLT-005 was present in both the retina and PECS in a dose-dependent manner (Figs. 5A, 5B). Therefore, in conjunction with the data in Figure 2E, we can conclude that CLT-005 was actively inhibiting Stat3 in the eye throughout the study.

We used multiplex analysis to examine the cytokine expression profile in the retina to determine whether CLT-005 mediated inhibition of Stat3 functions to negatively regulate the inflammatory pathway. We show that inflammatory cytokines are upregulated in the retina of STZ-diabetic rats treated with vehicle alone, and CLT-005 has a profound, dose-dependent effect on downregulating all examined cytokines in the retina (Fig. 6; Table). Importantly, we identify downregulation by CLT-005 of several cytokines that are upregulated in the ocular tissue of human patients with DR, including MCP-1, growth-regulated oncogene/keratinocyte chemoattractanct (GRO/KC), VEGF, IL-6, and IL-1β, and IL-2 (Fig. 6; Table). Therefore, these results suggest that orally administered CLT-005 decreases the levels of inflammatory cytokines in the retina, and this may be an important mechanism in the overall positive effect on slowing vision loss.

Discussion

In this study, we demonstrate that systemic Stat3 inhibition by the small molecule inhibitor CLT-005 delays and reduces STZ-diabetic rat vision loss in a dose-dependent manner. DR is a multifactorial disease with multiple pathogenic processes

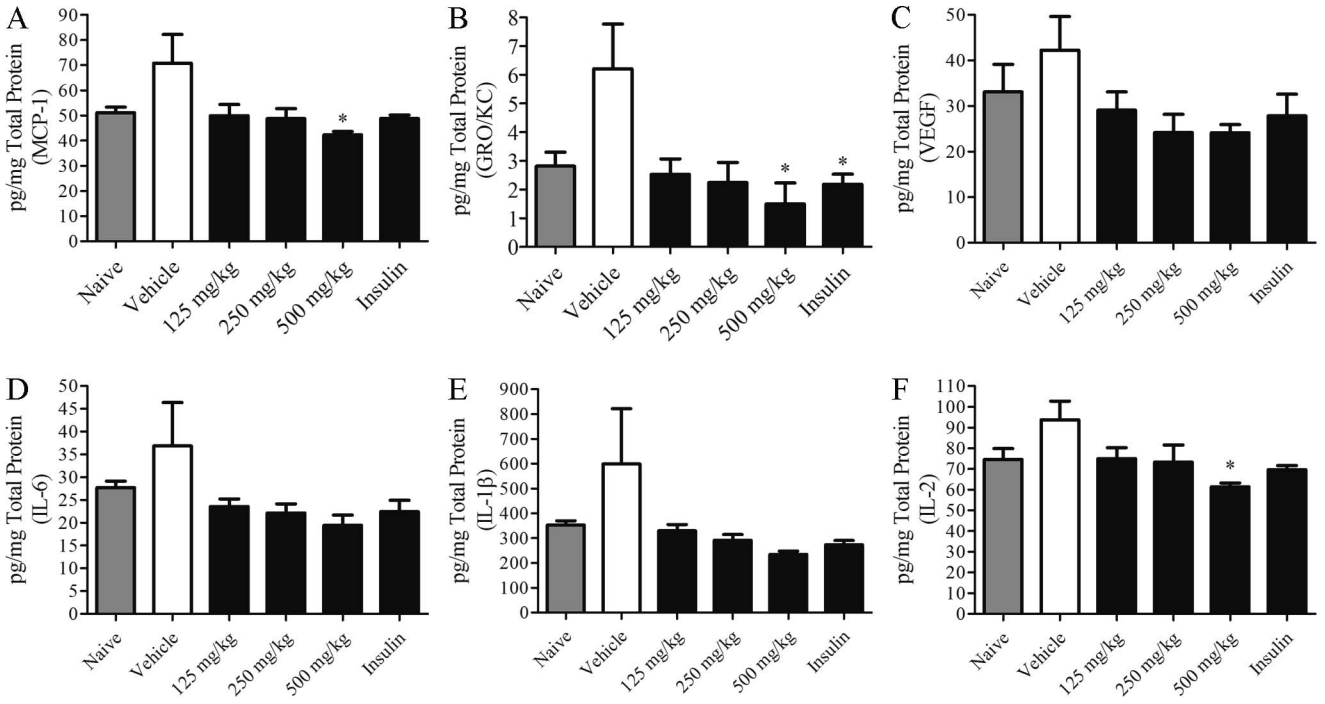

Figure 6. CLT-005 downregulates inflammatory mediators in STZ-diabetic rat eyes. Equal concentrations of protein from individual eyes were analyzed using a Bio Rad Bio-plex Pro Rat Cytokine group I 23-Plex Assay according to the manufacturer's protocol (see Materials and Methods; $n = 4$; mean ± SEM; $^*P < 0.05$; 1-way ANOVA with Tukey's posttest). The data presented in this figure is selected from more than 20 examined cytokines (see Table).

contributing to vision loss, and understanding the biochemical pathways and metabolic dysfunctions underlying DR is necessary for a better approach to drug design. However, potential therapies will only be deemed effective if they positively impact vision loss in patients. OKT measurements of visual function in diabetic animals offer a direct, clinically relevant, and translatable measure of DR disease progression and therapeutic intervention. Vision loss is seen across multiple rodent strains and rodent species following induction of diabetes by STZ treatment. Consistent with our analysis of vision loss in STZ-diabetic BN rats, STZ-diabetic Long Evans rats display a progressive loss in visual acuity and contrast sensitivity.[48] Similarly, in STZ-diabetic mice, visual acuity and contrast sensitivity are significantly reduced as early as 1 month post STZ.[49] Our data support these earlier studies, providing further evidence for STZ-diabetic rodents as viable models for

Table. Cytokine Levels in the Retina of CLT-005 Treated Diabetic Rats

Analyte	Naïve	Vehicle	125 mg/kg	250 mg/kg	500 mg/kg	Insulin
IL-1α	33.2 ± 2.78	45.1 ± 9.9	25.1 ± 4.7	27.9 ± 1.9	31.0 ± 6.7	27.4 ± 6.4
IL-4	9.3 ± 0.2	12.4 ± 3.0	9.6 ± 0.7	8.0 ± 0.3	8.3 ± 0.1	8.1 ± 0.7
IL-1β	353.1 ± 17.1	598.9 ± 222.7	329.6 ± 25.6	291.1 ± 23.9	234.7 ± 12.8	273.4 ± 17.3
IL-2	74.5 ± 5.2	93.8 ± 9.0	75.0 ± 5.3	73.3 ± 8.2	61.3 ± 1.9	69.6 ± 2.0
IL-6	27.7 ± 1.4	36.9 ± 9.6	23.6 ± 1.7	22.2 ± 2.0	19.4 ± 2.2	22.4 ± 2.5
IL-13	5.7 ± 0.5	9.7 ± 3.2	4.5 ± 0.7	4.9 ± 0.8	2.8 ± 0.1	4.1 ± 0.3
IL-10	104.1 ± 6.4	128.5 ± 23.2	106.8 ± 6.8	102.1 ± 8.6	91.7 ± 4.0	91.8 ± 13.7
IL-12 (p70)	15.4 ± 2.5	29.8 ± 7.9	16.3 ± 1.9	14.9 ± 3.7	10.8 ± 0.8	15.7 ± 1.0
IFNγ	27.5 ± 2.4	46.2 ± 14.0	30.9 ± 3.2	24.2 ± 5.0	16.6 ± 2.5	24.1 ± 0.9
IL-5	34.7 ± 2.4	41.3 ± 8.7	28.6 ± 0.8	33.3 ± 1.8	28.3 ± 1.8	28.0 ± 2.6
IL-17	8.4 ± 0.2	13.9 ± 4.4	7.9 ± 0.6	8.2 ± 0.6	7.0 ± 0.1	7.7 ± 0.6
IL-18	753.7 ± 22.5	771.1 ± 47.4	720.7 ± 63.0	746.2 ± 37.6	665.7 ± 16.5	710.1 ± 35.9
MCP-1	51.1 ± 2.2	70.8 ± 11.4	49.9 ± 4.4	48.7 ± 4.0	42.3 ± 1.4	48.8 ± 1.3
GRO-KC	2.8 ± 0.5	6.2 ± 1.6	2.5 ± 0.5	2.2 ± 0.6	1.5 ± 0.6	2.2 ± 0.4
VEGF	33.1 ± 6.0	42.3 ± 7.3	29.1 ± 4.0	24.2 ± 4.0	24.1 ± 1.8	27.9 ± 4.7
RANTES	47.5 ± 3.3	78.6 ± 27.6	44.8 ± 4.0	42.3 ± 2.7	34.2 ± 4.0	37.4 ± 2.7
EPO	139.8 ± 8.5	162.0 ± 29.5	120.0 ± 8.7	124.0 ± 4.0	122.5 ± 14.7	111.9 ± 7.5
IL-7	97.3 ± 11.4	128.6 ± 25.0	86.7 ± 10.3	85.5 ± 12.5	68.6 ± 3.8	73.3. ± 5.2
M-CSF	8.2 ± 1.3	13.7 ± 2.0	6.5 ± 1.0	5.6 ± 1.2	4.8 ± 0.2	5.8 ± 1.1
MIP-3α	8.0 ± 0.3	10.9 ± 2.8	7.0 ± 0.6	6.8 ± 0.3	6.5 ± 0.1	7.1 ± 0.5

All values are in pg/mg. MCP-1, monocyte chemotactic protein 1; GRO-KC, growth regulated oncogene/keratinocyte chemoattractant; RANTES, regulated on activation, normal T cell expressed and secreted; EPO, erythropoietin; M-CSF, macrophage colony-stimulating factor; MIP-3, macrophage inflammatory protein-3.

Investigative Ophthalmology & Visual Science

the study of DR-dependent vision loss and therapeutic intervention.

We identified the following three major pathogenic processes that are ameliorated through chronic and systemic Stat3 inhibition and that may impact vision loss separately or in conjunction: (1) hyperglycemia, (2) cataract formation, and (3) upregulation of inflammatory and angiogenic molecular mediators. The diabetic hyperglycemic environment is considered a risk factor for cataract formation, inflammation, and vascular defects; therefore, it is difficult to determine whether this process alone is impacted by the regulation of Stat3 or if targeting Stat3 activation has independent effects on these processes. However, visual acuity and contrast thresholds are similar between the 500 mg/kg CLT-005 and insulin-treatment groups despite the lack of hyperglycemia in the insulin group. This suggests that CLT-005 mediated Stat3 inhibition has additional therapeutic effects.

DM patients have a fivefold higher incidence of cataracts when compared with the nondiabetic population,[57] and lens opacity has been cited as a cause of vision loss in diabetic patients.[58,59] However, although cataract severity correlates with increased visual deficits, the presence of cataracts are not necessary for diabetic patients to experience vision loss.[60] Our finding that visual acuity can be partially segregated from an influence by cataracts is consistent with this finding in human patients and previous findings in diabetic rodents.[48,50]

Chronic inflammation is prevalent in both type I and type II diabetes and may be a result of the increased presence of reactive oxygen species as a result of hyperglycemia.[61,62] In addition to the data presented here, a number of studies have linked specific inflammatory cytokines to DR. IL-1β is upregulated in diabetic rat retina during the acute phase of the disease.[61–64] TNFα is detected at high levels in the vitreous of diabetic patients and animal models of diabetes.[65–69] Additional cytokines now understood to be associated with DR through animal models and clinical evidence in the eyes of diabetic patients include the growth-related oncogene, IL-6, MCP-1, and IL-8.[70–73] Previous studies have shown that Stat3 activity drives the expression of inflammatory cytokines in the retinas of diabetic mice.[35–38] Importantly, we show that the high dose of the Stat3 inhibitor CLT-005 in STZ-diabetic rats decreases many of the inflammatory cytokines below the levels seen with insulin treatment and that CLT-005 provides therapeutic benefit to delay and reduce vision loss similar to insulin treatment despite ongoing hyperglycemia in CLT-005-treated STZ-diabetic rats. Thus, similar to previous studies, this study suggests that retinal inflammation is a primary mechanism driving vision loss in DR.[19,64] We do not know whether any possible effect of CLT-005 on glucose levels is related to the mechanism through which CLT-005 decreases inflammation.

The anti-VEGF treatments clinically available require intravitreal injections that are associated with high costs and side effects. Furthermore, these therapies require relatively frequent injections, which may be prohibitive to long-term care because of compliance. In addition to targeting the Stat3 pathway, CLT-005 offers the distinct therapeutic advantage of being a small molecule that effectively reaches the retina following systemic administration. The major hurdle to advancing CLT-005 to clinical studies is that it has low solubility (<0.006 mg/ml) and requires a large daily oral dose (~500 mg/kg) to elicit a therapeutic effect. The volume of distribution has been determined from tail vein injections to be 22 L/kg with a half-life of 0.011 hours for CLT-005. Therefore, CLT-005 is not ideal in its present form. We are currently exploring increasing the solubility and bioavailability by spray drying CLT-005 in the presence of various surfactants, and in vivo studies to assess the pharmacokinetic properties of the spray dried material are ongoing. Regardless of the outcome of these efforts, the data in this article strengthen the logic that Stat3 is a viable therapeutic target, and new drugs targeting Stat3 could provide important second-line therapies for DR in the clinic.

Acknowledgments

Supported by the National Institutes of Health and National Eye Institute Small Business Innovation Research Program Grant 2R44EY018989-02 awarded to R.A.F.

Disclosure: **P.A. Vanlandingham**, None; **D.J. Nuno**, None; **A.B. Quiambao**, None; **E. Phelps**, None; **R.A. Wassel**, None; **J.-X. Ma**, None; **K.M. Farjo**, None; **R.A. Farjo**, None

References

1. Vaz JA, Patnaik A. Diabetes mellitus: exploring the challenges in the drug development process. *Perspect Clin Res*. 2012; 3109–3112.
2. Klein R, Knudtson MD, Lee KE, Gangnon R, Klein BE. The Wisconsin Epidemiologic Study of Diabetic Retinopathy: XXII the twenty-five-year progression of retinopathy in persons with type 1 diabetes. *Ophthalmology*. 2008;115:1859–1868.
3. Ko F, Vitale S, Chou CF, Cotch MF, Saaddine J, Friedman DS. Prevalence of nonrefractive visual impairment in US adults and associated risk factors, 1999-2002 and 2005-2008. *JAMA*. 2012;308:2361–2368.
4. Aiello LM. Preserving human vision: eliminating blindness from diabetes mellitus. *J Am Optom Assoc*. 1998;69:690–692.
5. Fong DS, Aiello L, Gardner TW, et al. Diabetic retinopathy. *Diabetes Care*. 2003;26:226–229.
6. Andrade LC, Souza GS, Lacerda EM, et al. Influence of retinopathy on the achromatic and chromatic vision of patients with type 2 diabetes. *BMC Ophthalmol*. 2014;14: 104.
7. Arend O, Remky A, Evans D, Stüber R, Harris A. Contrast sensitivity loss is coupled with capillary dropout in patients with diabetes. *Invest Ophthalmol Vis Sci*. 1997;38:1819–1824.
8. Ashton N. Arteriolar involvement in diabetic retinopathy. *Br J Ophthalmol*. 1953;37:282–292.
9. Di Leo MA, Caputo S, Falsini B, Porciatti V, Greco AV, Ghirlanda G. Presence and further development of retinal dysfunction after 3-year follow up in IDDM patients without angiographically documented vasculopathy. *Diabetologia*. 1994;37:911–916.
10. Harris A, Arend O, Danis RP, Evans D, Wolf S, Martin BJ. Hyperoxia improves contrast sensitivity in early diabetic retinopathy. *Br J Ophthalmol*. 1996;80:209–213.
11. Mizutani M, Kern TS, Lorenzi M. Accelerated death of retinal microvascular cells in human and experimental diabetic retinopathy. *J Clin Invest*. 1996;97:2883–2890.
12. Sokol S, Moskowitz A, Skarf B, Evans R, Molitch M, Senior B. Contrast sensitivity in diabetics with and without background retinopathy. *Arch Ophthalmol*. 1985;103:51–54.
13. Barber AJ, Lieth E, Khin SA, Antonetti DA, Buchanan AG, Gardner TW. Neural apoptosis in the retina during experimental and human diabetes. Early onset and effect of insulin. *J Clin Invest*. 1998;102:783–791.
14. Cheung N, Mitchell P, Wong TY. Diabetic retinopathy. *Lancet*. 2010;376:124–136.
15. Cunha-Vaz J, Ribeiro L, Lobo C. Phenotypes and biomarkers of diabetic retinopathy. *Prog Retin Eye Res*. 2014;41:90–111.
16. Decanini A, Karunadharma PP, Nordgaard CL, Feng X, Olsen TW, Ferrington DA. Human retinal pigment epithelium proteome changes in early diabetes. *Diabetologia*. 2008;51: 1051–1061.

17. Joussen AM, Poulaki V, Le ML, et al. A central role for inflammation in the pathogenesis of diabetic retinopathy. *FASEB J*. 2004;18:1450–1452.
18. Powell EU, Field R. Diabetic retinopathy and rheumatoid arthritis. *Lancet*. 1964;284:17–18.
19. Tang J, Kern TS. Inflammation in diabetic retinopathy. *Prog Retin Eye Res*. 2011;30:343–358.
20. Yang LP, Sun HL, Wu LM, et al. Baicalein reduces inflammatory process in a rodent model of diabetic retinopathy. *Invest Ophthalmol Vis Sci*. 2009;50:2319–2327.
21. Aiello LP, Edwards AR, Beck RW, et al. Factors associated with improvement and worsening of visual acuity 2 years after focal/grid photocoagulation for diabetic macular edema. *Ophthalmology*. 2010;117:946–953.
22. Elman MJ, Aiello LP, Beck RW, et al.; Diabetic Retinopathy Clinical Research Network. Randomized trial evaluating ranibizumab plus prompt or deferred laser or triamcinolone plus prompt laser for diabetic macular edema. *Ophthalmology*. 2010;117:1064–1077.e35.
23. Scott IU, Edwards AR, Beck RW, et al.; Diabetic Retinopathy Clinical Research Network. A phase II randomized clinical trial of intravitreal bevacizumab for diabetic macular edema. *Ophthalmology*. 2007;114:1860–1867.
24. Nguyen QD, Tatlipinar S, Shah SM, et al. Vascular endothelial growth factor is a critical stimulus for diabetic macular edema. *Am J Ophthalmol*. 2006;142:961–969.
25. Regnier S, Malcolm W, Allen F, Wright J, Bezlyak V. Efficacy of anti-VEGF and laser photocoagulation in the treatment of visual impairment due to diabetic macular edema: a systematic review and network meta-analysis. *PLoS One*. 2014;9:e102309.
26. Du Z, Shen Y, Yang W, Mecklenbrauker I, Neel BG, Ivashkiv LB. Inhibition of IFN-alpha signaling by a PKC- and protein tyrosine phosphatase SHP-2-dependent pathway. *Proc Natl Acad Sci U S A*. 2005;102:10267–10272.
27. Sansone P, Bromberg J. Targeting the interleukin-6/Jak/stat pathway in human malignancies. *J Clin Oncol*. 2012;30:1005–1014.
28. Tian SS, Tapley P, Sincich C, Stein RB, Rosen J, Lamb P. Multiple signaling pathways induced by granulocyte colony-stimulating factor involving activation of JAKs, STAT5, and/or STAT3 are required for regulation of three distinct classes of immediate early genes. *Blood*. 1996;88:4435–4444.
29. Turkson J, Bowman T, Adnane J, et al. Requirement for Ras/Rac1-mediated p38 and c-Jun N-terminal kinase signaling in Stat3 transcriptional activity induced by the Src oncoprotein. *Mol Cell Biol*. 1999;19:7519–7528.
30. Escobar T, Yu CR, Muljo SA, Egwuagu CE. STAT3 activates miR-155 in Th17 cells and acts in concert to promote experimental autoimmune UveitisSTAT3/miR-155 axis promotes Th17 development and EAU. *Invest Ophthalmol Vis Sci*. 2013;54:4017–4025.
31. Okamoto T, Ozawa Y, Kamoshita M, et al. The neuroprotective effect of rapamycin as a modulator of the mTOR-NF-κB axis during retinal inflammation. *PLoS One*. 2016;11:e0146517.
32. Wong M, Li Y, Li S, et al. Therapeutic retrobulbar inhibition of STAT3 protects ischemic retina ganglion cells. *Mol Neurobiol*. 2015;52:1364–1377.
33. Yu C-R, Lee YS, Mahdi RM, Surendran N, Egwuagu CE. Therapeutic targeting of STAT3 (signal transducers and activators of transcription 3) pathway inhibits experimental autoimmune uveitis. *PLoS One*. 2012;7:e29742.
34. Yang Z, Wang H, Jiang Y, Hartnett ME. VEGFA activates erythropoietin receptor and enhances VEGFR2-mediated pathological angiogenesis. *Am J Pathol*. 2014;184:1230–1239.
35. VanGuilder HD, Bixler GV, Kutzler L, et al. Multi-modal proteomic analysis of retinal protein expression alterations in a rat model of diabetic retinopathy. *PLoS One*. 2011;6:e16271.
36. Li P, Xu X, Zheng Z, Zhu B, Shi Y, Liu K. Protective effects of rosiglitazone on retinal neuronal damage in diabetic rats. *Curr Eye Res*. 2011;36:673–679.
37. Chen Y, Wang JJ, Li J, et al. Activating transcription factor 4 mediates hyperglycaemia-induced endothelial inflammation and retinal vascular leakage through activation of STAT3 in a mouse model of type 1 diabetes. *Diabetologia*. 2012;55:2533–2545.
38. Al-Shabrawey M, Bartoli M, El-Remessy AB, et al. Role of NADPH oxidase and Stat3 in statin-mediated protection against diabetic retinopathy. *Invest Ophthalmol Vis Sci*. 2008;49:3231–3238.
39. Li J, Wang JJ, Yu Q, Chen K, Mahadev K, Zhang SX. Inhibition of reactive oxygen species by lovastatin downregulates vascular endothelial growth factor expression and ameliorates blood-retinal barrier breakdown in db/db mice: role of NADPH oxidase 4. *Diabetes*. 2010;59:1528–1538.
40. Lenzen S. The mechanisms of alloxan- and streptozotocin-induced diabetes. *Diabetologia*. 2008;51:216–226.
41. Szkudelski T. The mechanism of alloxan and streptozotocin action in B cells of the rat pancreas. *Physiol Res*. 2001;50:537–546.
42. Beauchemin ML, Leuenberger PM, Babel J. Retinal capillary basement membrane thickness in spiny mice (*Acomys cahirinus*) with induced and spontaneous diabetes. *Invest Ophthalmol*. 1975;14:560–562.
43. Gastinger MJ, Singh RS, Barber AJ. Loss of cholinergic and dopaminergic amacrine cells in streptozotocin-diabetic rat and Ins2Akita-diabetic mouse retinas. *Invest Ophthalmol Vis Sci*. 2006;47:3143–3150.
44. Kim JH, Kim JH, Jun HO, Yu YS, Kim KW. Inhibition of protein kinase C delta attenuates blood-retinal barrier breakdown in diabetic retinopathy. *Am J Pathol*. 2010;176:1517–1524.
45. Martin PM, Roon P, Van Ells TK, Ganapathy V, Smith SB. Death of retinal neurons in streptozotocin-induced diabetic mice. *Invest Ophthalmol Vis Sci*. 2004;45:3330–3336.
46. Robison WG Jr, McCaleb ML, Feld LG, Michaelis OE IV, Laver N, Mercandetti M. Degenerated intramural pericytes ('ghost cells') in the retinal capillaries of diabetic rats. *Curr Eye Res*. 1991;10:339–350.
47. Alam NM, Mills MC IV, Wong AA, Douglas RM, Szeto HH, Prusky GT. A mitochondrial therapeutic reverses visual decline in mouse models of diabetes. *Dis Models Mech*. 2015;8:701–710.
48. Aung MH, Kim MK, Olson DE, Thule PM, Pardue MT. Early visual deficits in streptozotocin-induced diabetic Long Evans rats. *Invest Ophthalmol Vis Sci*. 2013;54:1370–1377.
49. Aung MH, Park HN, Han MK, et al. Dopamine deficiency contributes to early visual dysfunction in a rodent model of type 1 diabetes. *J Neurosci*. 2014;34:726–736.
50. Kirwin SJ, Kanaly ST, Hansen CR, Cairns BJ, Ren M, Edelman JL. Retinal gene expression and visually evoked behavior in diabetic Long Evans rats. *Invest Ophthalmol Vis Sci*. 2011;52:7654–7663.
51. Bhasin D, Cisek K, Pandharkar T, et al. Design, synthesis, and studies of small molecule STAT3 inhibitors. *Bioorg Med Chem Lett*. 2008;18:391–395.
52. Fuh B, Sobo M, Cen L, et al. LLL-3 inhibits STAT3 activity, suppresses glioblastoma cell growth and prolongs survival in a mouse glioblastoma model. *Br J Cancer*. 2009;100:106–112.
53. Xu Q, Qaum T, Adamis AP. Sensitive blood-retinal barrier breakdown quantitation using Evans Blue. *Invest Ophthalmol Vis Sci*. 2001;42:789–794.

Investigative Ophthalmology & Visual Science

54. Farjo R, Peterson WM, Naash MI. Expression profiling after retinal detachment and reattachment: a possible role for aquaporin-0. *Invest Ophthalmol Vis Sci*. 2008;49:511–521.
55. Prusky GT, Alam NM, Beekman S, Douglas RM. Rapid quantification of adult and developing mouse spatial vision using a virtual optomotor system. *Invest Ophthalmol Vis Sci*. 2004;45:4611–4616.
56. Muranov K, Poliansky N, Winkler R, Rieger G, Schmut O, Horwath-Winter J. Protection by iodide of lens from selenite-induced cataract. *Ger J Ophthalmol*. 2004;242:146–151.
57. Obrosova IG, Chung SSM, Kador PF. Diabetic cataracts: mechanisms and management. *Diabetes Metab Res Rev*. 2010;26:172–180.
58. Hardy KJ, Scarpello JH, Foster DH, Moreland JD. Effect of diabetes associated increases in lens optical density on colour discrimination in insulin dependent diabetes. *Br J Ophthalmol*. 1994;78:754–756.
59. Kessel L, Alsing A, Larsen M. Diabetic versus non-diabetic colour vision after cataract surgery. *Br J Ophthalmol*. 1999; 83:1042–1045.
60. Bron AJ, Cheng H. Cataract and retinopathy: screening for treatable retinopathy. *Clin Endocrinol Metab*. 1986;15:971–999.
61. Liu Y, Biarnés Costa M, Gerhardinger C. IL-1beta is upregulated in the diabetic retina and retinal vessels: cell-specific effect of high glucose and IL-1beta autostimulation. *PLoS One*. 2012;7:e36949.
62. Scuderi S, Dámico AG, Federico C, et al. Different retinal expression patterns of IL-1alpha, IL-1beta, and their receptors in a rat model of type 1 STZ-induced diabetes. *J Mol Neurosci*. 2015;56:431–439.
63. Gerhardinger C, Costa MB, Coulombe MC, Toth I, Hoehn T, Grosu P. Expression of acute-phase response proteins in retinal Müller cells in diabetes. *Invest Ophthalmol Vis Sci*. 2005;46:349–357.
64. Kern TS. Contributions of inflammatory processes to the development of the early stages of diabetic retinopathy. *Exp Diabetes Res*. 2007;2007:95103.
65. Abu el Asrar AM, Maimone D, Morse PH, Gregory S, Reder AT. Cytokines in the vitreous of patients with proliferative diabetic retinopathy. *Am J Ophthalmol*. 1992;114:731–736.
66. Demircan N, Safran BG, Soylu M, Ozcan AA, Sizmaz S. Determination of vitreous interleukin-1 (IL-1) and tumour necrosis factor (TNF) levels in proliferative diabetic retinopathy. *Eye (Lond)*. 2006;20:1366–1369.
67. Joussen AM, Doehmen S, Le ML, et al. TNF-alpha mediated apoptosis plays an important role in the development of early diabetic retinopathy and long-term histopathological alterations. *Mol Vis*. 2009;15:1418–1428.
68. Joussen AM, Poulaki V, Mitsiades N, et al. Nonsteroidal anti-inflammatory drugs prevent early diabetic retinopathy via TNF-alpha suppression. *FASEB J*. 2002;16:438–440.
69. Yuuki T, Kanda T, Kimura Y, et al. Inflammatory cytokines in vitreous fluid and serum of patients with diabetic vitreoretinopathy. *J Diabetes Complications*. 2001;15:257–259.
70. Bromberg-White JL, Glazer L, Downer R, Furge K, Boguslawski E, Duesbery NS. Identification of VEGF-independent cytokines in proliferative diabetic retinopathy vitreous. *Invest Ophthalmol Vis Sci*. 2013;54:6472–6480.
71. Lange CA, Stavrakas P, Luhmann UF, et al. Intraocular oxygen distribution in advanced proliferative diabetic retinopathy. *Am J Ophthalmol*. 2011;152:406–412.e3.
72. Limb GA, Webster L, Soomro H, Janikoun S, Shilling J. Platelet expression of tumour necrosis factor-alpha (TNF-alpha), TNF receptors and intercellular adhesion molecule-1 (ICAM-1) in patients with proliferative diabetic retinopathy. *Clin Exp Immunol*. 1999;118:213–218.
73. Schoenberger SD, Kim SJ, Sheng J, Rezaei KA, Lalezary M, Cherney E. Increased prostaglandin E2 (PGE2) levels in proliferative diabetic retinopathy, and correlation with VEGF and inflammatory cytokines. *Invest Ophthalmol Vis Sci*. 2012;53:5906–5911.

Investigative Ophthalmology & Visual Science